Passive Mechanical Behavior of Human Neutrophils: Power-Law Fluid

Mientao A. Tsai,* Robert S. Frank,‡ and Richard E. Waugh*

*Department of Biophysics, University of Rochester School of Medicine and Dentistry, Rochester, New York, and ‡Applied Research Department, Coulter Corporation, Hialeah, Florida, USA

ABSTRACT   The mechanical behavior of the neutrophil plays an important role in both the microcirculation and the immune system. Several laboratories in the past have developed mechanical models to describe different aspects of neutrophil deformability. In this study, the passive mechanical properties of normal human neutrophils have been further characterized. The cellular mechanical properties were assessed by single cell micropipette aspiration at fixed aspiration pressures. A numerical simulation was developed to interpret the experiments in terms of cell mechanical properties based on the Newtonian liquid drop model (Yeung and Evans, $Biophys. J.$, 56:139–149, 1989). The cytoplasmic viscosity was determined as a function of the ratio of the initial cell size to the pipette radius, the cortical tension, aspiration pressure, and the whole cell aspiration time. The cortical tension of passive neutrophils was measured to be about 2.7×10^{-5} N/m. The apparent viscosity of neutrophil cytoplasm was found to depend on aspiration pressure, and ranged from ~ 500 Pa·s at an aspiration pressure of 98 Pa (1.0 cm H_2O) to ~ 50 Pa·s at 882 Pa (9.0 cm H_2O) when tested with a 4.0-μm pipette. These data provide the first documentation that the neutrophil cytoplasm exhibits non-Newtonian behavior. To further characterize the non-Newtonian behavior of human neutrophils, a mean shear rate $\dot{\gamma}_m$ was estimated based on the numerical simulation. The apparent cytoplasmic viscosity appears to decrease as the mean shear rate increases. The dependence of cytoplasmic viscosity on the mean shear rate can be approximated as a power-law relationship described by $\mu = \mu_c(\dot{\gamma}_m/\dot{\gamma}_c)^{-b}$, where μ is the cytoplasmic viscosity, $\dot{\gamma}_m$ is the mean shear rate, μ_c is the characteristic viscosity at characteristic shear rate $\dot{\gamma}_c$, and b is a material coefficient. When $\dot{\gamma}_c$ was set to 1 s^{-1}, the material coefficients for passive neutrophils were determined to be $\mu_c = 130 \pm 23$ Pa·s and $b = 0.52 \pm 0.09$ for normal neutrophils. The power-law approximation has a remarkable ability to reconcile discrepancies among published values of the cytoplasmic viscosity measured using different techniques, even though these values differ by nearly two orders of magnitude. Thus, the power-law fluid model is a promising candidate for describing the passive mechanical behavior of human neutrophils in large deformation. It can also account for some discrepancies between cellular behavior in single-cell micromechanical experiments and predictions based on the assumption that the cytoplasm is a simple Newtonian fluid.

INTRODUCTION

Neutrophils constitute one of the most important defense systems in the human body to combat disease. In the course of carrying out their function, they must undergo large deformations as they negotiate the small apertures in the tissues and the microvasculature. Thus, their mechanical behavior plays an important role in both the microcirculation and the immune system. Over the last two decades, a variety of techniques have been developed and applied to quantify leukocyte mechanical properties. Micropipette manipulation is the most widely used and successful technique among them. The reported values of cytoplasmic viscosity range from 135 Pa·s (Needham and Hochmuth, 1990; Hochmuth and Needham, 1990) to 200 Pa·s (Evans and Yeung, 1989) when measured by micropipette aspiration at 20°C. In one laboratory, the cytoplasmic viscosity was reported to be as low as 30 Pa·s (Dong et al., 1988). An analogous apparatus, micropore filtration, yielded values of cytoplasmic viscosity of 60 to 160 Pa·s (Frank and Tsai, 1990). In contrast to these small values of viscosity, magnetic probe experiments indicate that the cytoplasmic viscosity is shear rate dependent and ranges

from 1200 Pa·s at a shear rate of 0.003 s^{-1} to 2700 Pa·s at 0.001 s^{-1} at 37°C (Valberg and Albertini, 1985).

A great deal of effort has also been made to develop mechanical models of passive granulocytes. The first mechanical model described the granulocyte under small deformations as a standard viscoelastic solid: a principal elastic element in parallel with a Maxwell fluid element (Schmid-Schönbein et al., 1981; Chien and Sung, 1984). The principal elastic element represents an ultimate static limit to the cellular deformation. However, observations of neutrophils undergoing large deformations showed that such a static limit was not obtained, and so the Newtonian liquid drop model was introduced by Evans and colleagues (Evans and Kukan, 1984; Yeung and Evans, 1989). It describes the neutrophil as a Newtonian liquid core enclosed in a cortical membrane with a persistent ("surface") tension of about 3.5×10^{-5} N/m (Evans and Yeung, 1989). It predicts that the persistent cortical tension results in a threshold pressure for granulocytes to enter a micropipette and that once the threshold pressure is exceeded, the deformation of the cell into the micropipette is a continuous process with no static limitation. This prediction is consistent with the observations in whole cell aspiration experiments (Hochmuth and Needham, 1990; Needham and Hochmuth, 1990). Since its inception, the liquid drop model has been refined to include the effect of energy dissipation within the surface cortex (Yeung and Evans,

1989). Experimental measurements indicate that the effect is insignificant compared to that of the liquid core, provided the pipette diameter is large (>3.5 μm) and aspiration pressure is high (20 times above the threshold pressure). To address the elastic-like behavior of human neutrophils observed in rapid deformation experiments, the Maxwell fluid model was recently proposed in which an elastic element was added in series with the viscous element in the liquid core (Dong et al., 1988; Skalak et al., 1990). Numerical simulations based on this model indicate that the cellular mechanical properties must vary with the state of cell deformation to match experimental data (Dong et al., 1991), that is, the model parameters are deformation dependent. Thus, this model does not appear to be consistent with the actual behavior of neutrophils.

In developing a mechanical model, cellular structure should be taken into account as well as cell mechanical response. In general, the neutrophil can be simplified as a system of three components: the cortical membrane, a lobular segmented nucleus, and the cytoplasm. The cortical membrane comprises the lipid bilayer with a supporting filamentous network (Sheterline and Rickard, 1989; Yeung and Evans, 1989). The lipid bilayer has about 110% to 200% extra surface area stored in forms of ruffles and folds (Lichtman and Kearney, 1976; Schmid-Schönbein et al., 1980; Evans and Kukan, 1984; Ting-Beall et al., 1993) which makes it possible for human neutrophils to undergo very large deformations without being constrained by the fixed surface area of the bilayer. The cytoplasm is the predominant component of the cell and occupies about 78% of the total cell volume (Schmid-Schönbein et al., 1980). The constituents of the cytoplasm include water, granules, proteins, and solutes with three classes of dynamic filamentous systems (actin filaments, microtubules, and intermediate filaments) permeating the cytoplasmic space to form the cytoskeleton (Janmey, 1991). The size of the granules ranges from 0.1 to 0.5 μm in diameter (Bainton, 1988; Newburger and Parmley, 1991), and their volume accounts for ~15% of the total cell volume (Schmid-Schönbein et al., 1980). Other particulates in the cytoplasm include mitochondria, which fill about 0.6% of total cell volume. With these structural characteristics, particularly the presence of filamentous components, non-Newtonian behavior of the cytoplasm would be expected.

Despite intensive efforts, the passive mechanical behavior of the human neutrophil has still not been satisfactorily described. For instance, current models fail to account for the difference in cytoplasmic viscosity (as much as two orders of magnitude) among published values obtained using different methods and in different laboratories. Based on the experimental studies described in this article, we propose that many of the discrepancies in the literature can be accounted for by recognizing that the cytoplasmic viscosity is shear rate dependent. Thus, the current study provides a basis and motivation for developing a more true-to-life mechanical model that accounts for the non-Newtonian behavior of passive human neutrophils.

MATERIALS AND METHODS

Experimental buffer

HEPES (N-2-hydroxyethylpiperazine-N'-2-ethanesulfonic acid)- buffered saline solution excluding Ca^{2+} and Mg^{2+} was used in our experiments. It consisted of NaCl (135.8 mM), KCl (4.8 mM), HEPES (11.3 mM), and HEPES sodium salt (9.3 mM), glucose (1 g/liter). Streptomycin sulfate (105 units/ml) and penicillin-G potassium salt (95.4 units/ml) were added to the buffer to retard bacteria growth. The osmolality and pH were adjusted to 290 ± 5 mOsm/kg and 7.40 ± 0.05, respectively. All chemicals were purchased from Sigma Chemical Company (St. Louis, MO). Before the experiment, bovine serum albumin (Sigma Chemical Company) (2 g/liter) was added to the buffer. The buffer was degassed and filtered through a 0.22-μm Millex-GS filter (Millipore Corporation, Bedford, MA). Autologous plasma (10% v/v) was mixed into the cell suspension buffer to reduce cell adhesion.

Neutrophil collection

About 10 ml whole blood was collected in a sterile vacuum tube with sodium heparin as the anticoagulant (Vacutainer; Becton Dickson, Rutherford, NJ) by venipuncture from healthy adult donors. The blood was allowed to cool to room temperature over a period of 25 min. Neutrophils were separated from whole blood with a Ficoll-Hypaque density gradient (Mono-Poly Resolving Medium; Flow Laboratories, Inc., McLean, VA). The sample was spun in a swinging bucket rotor centrifuge for 30 min at 1500 rpm (1000 × g). Collected neutrophils were washed twice and suspended in fresh HEPES buffer at a concentration of ~10^5 cells/ml.

Micropipette preparation

Micropipettes were pulled with a vertical pipette puller (Model 700C; David Kopf Instruments, Tujunga, CA) and fractured to the desired internal diameters with a microforge under a microscope. The surface of the pipettes was siliconized with 1% SurfaSil (Pierce Chemical Company, Rockford, IL). Internal diameters of the pipettes were determined from the insertion depth of a gold-coated probe that had been calibrated with a scanning electron microscope. Pipette sizes were chosen in a range of 4.0 to 5.5 μm. When used for an experiment, pipettes were filled with isotonic buffer with a specially designed pipette filler.

Experimental apparatus

Neutrophils were suspended in a U-shaped microchamber on the microscope stage. The pipette was inserted into the chamber and controlled by a micromanipulator. A single passive neutrophil was sucked into the pipette with a fixed aspiration pressure. The aspiration pressure was generated by displacing a hydrostatic reservoir and ranged from 98 to 882 Pa with an accuracy of ~1 Pa. A reference reservoir was used to locate the "zero" aspiration pressure. The process of the cell aspiration was observed on a TV monitor and was videotaped. The videotape was analyzed on a computer imaging system (MaxVision AT-1; Datacube, Peabody, MA).

THEORETICAL ANALYSIS AND NUMERICAL SIMULATION

To interpret the whole cell aspiration experiments in terms of the intrinsic cellular mechanical properties, a numerical simulation was carried out based on the Newtonian liquid

drop model. The shear rate of the cytoplasmic flow was calculated to facilitate a further assessment of possible non-Newtonian behavior of the neutrophil cytoplasm.

Basic assumptions

The cytoplasmic flow occurred at a very low Reynolds number (Re < 10^{-9}). Based on the experimental observations as shown in Fig. 1, the cytoplasmic flow was assumed to be axisymmetric, and the cell body outside the micropipette was spherical. The cortical membrane was assumed to offer no resistance to deformation except for a constant "surface" tension. The cytoplasm was approximated as an isotropic and incompressible Newtonian fluid. To further simplify the analysis, the cytoplasmic flow inside the pipette was assumed to be a plug flow. Viscous energy dissipation in the suspending medium was neglected since the viscosity of suspension buffer was less than that of the cytoplasm by a factor of 10^{-5}.

Governing equations and boundary conditions

The basic governing equations for the cytoplasmic flow included equations of continuity and conservation of momentum:

$$\nabla \cdot \mathbf{V} = 0, \tag{1}$$

$$\mu \nabla^2 \mathbf{V} = \nabla p \tag{2}$$

where $\mathbf{V}$ is the velocity vector, μ is the cytoplasmic viscosity, and p is the hydrostatic pressure.

A spherical coordinate system (r, θ, φ) was selected to formulate the problem. Since the cytoplasmic flow was incompressible and symmetric about the azimuthal axis φ, it was convenient to satisfy Eq. 1 by introducing a stream function $\psi(r, \theta)$ such that

$$V_r = -\frac{1}{r^2 \sin \theta} \frac{\partial \psi}{\partial \theta}, \tag{3}$$

$$V_\theta = \frac{1}{r \sin \theta} \frac{\partial \psi}{\partial r} \tag{4}$$

where V_r and V_θ are velocity components in r and θ directions, respectively. From Eq. 2, the stream function $\psi(r, \theta)$ satisfies
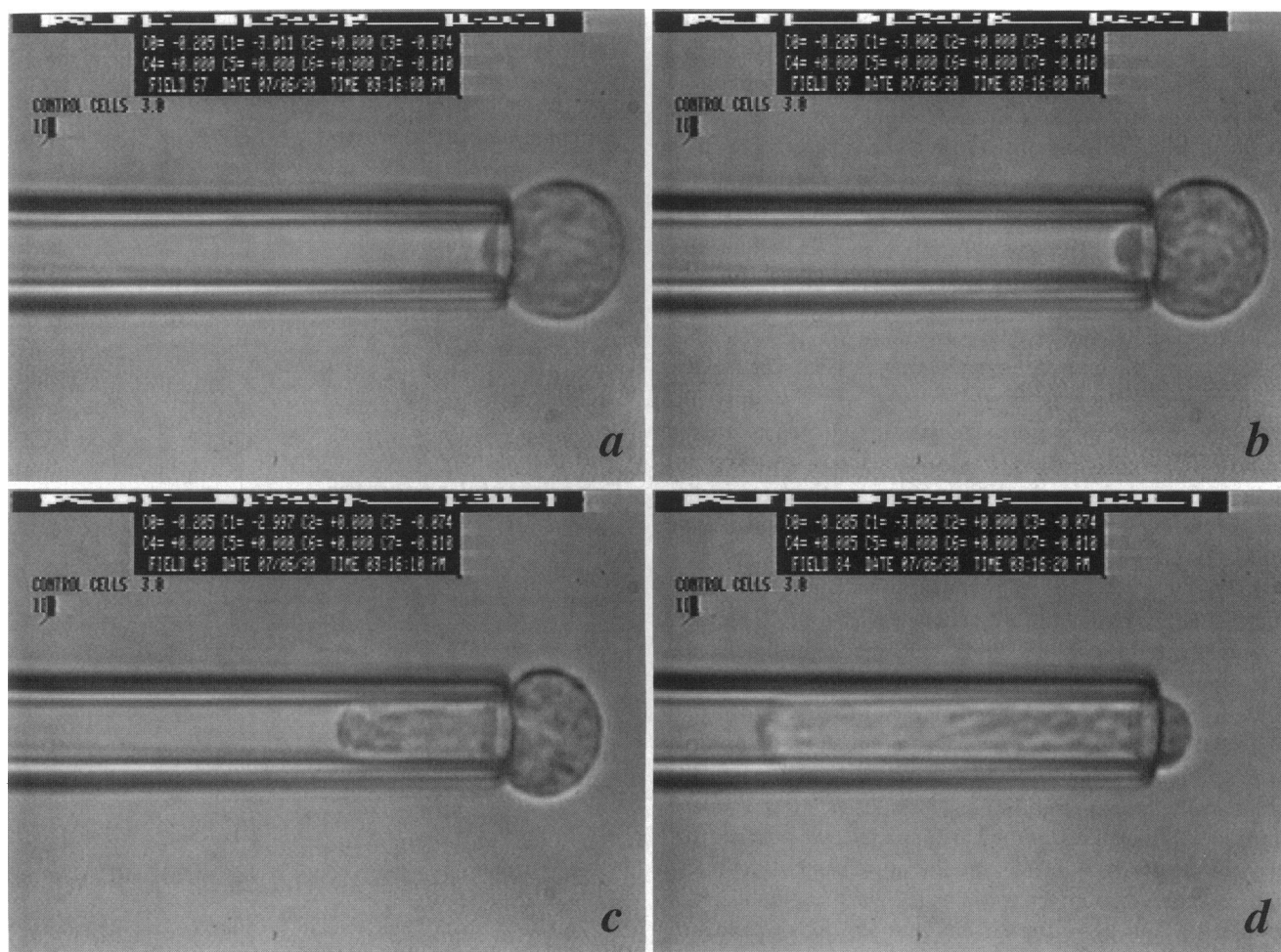
$$E^4 \psi = 0 \tag{5}$$

FIGURE 1 Micrographs of cell aspiration process. (*a*) initial response to a step aspiration pressure; (*b*) cell projection formed into a hemisphere; (*c*) cell partially drawn into the pipette; (*d*) cell fully aspirated into the pipette.

where the operator E^2 was defined as

$$E^2 = \frac{\partial^2}{\partial r^2} + \frac{1 - \zeta^2}{r^2} \frac{\partial^2}{\partial \zeta^2} \tag{6}$$

and $\zeta = \cos \theta$.

The general solution to Eq. 5 is well established (Lamb, 1945; Happel and Brenner, 1983):

$$\psi = \sum_{n=2}^{\infty} (A_n r^n + C_n r^{n+2}) I_n(\zeta) \tag{7}$$

where A_n and C_n are coefficients to be determined by boundary conditions, and $I_n(\zeta)$ are Gegenbauer functions of the first kind, defined by

$$I_n(\zeta) = \frac{P_{n-2}(\zeta) - P_n(\zeta)}{2n - 1} \tag{8}$$

and $P_n(\zeta)$ are Legendre polynomials. Based on the previous assumptions, stress boundary conditions were formulated as the following:

$$\sigma_{r\theta} = 0, \tag{9}$$

$$\sigma_{rr} = \begin{cases} -\left(p_a + \dfrac{2T}{R}\right) & \zeta_p + \epsilon < \zeta \le 1 \\ -k & \zeta_p - \epsilon \le \zeta \le \zeta_p + \epsilon \\ -\left(p_p + \dfrac{2T}{R_f}\right) & -1 \le \zeta < \zeta_p - \epsilon \end{cases} \tag{10}$$

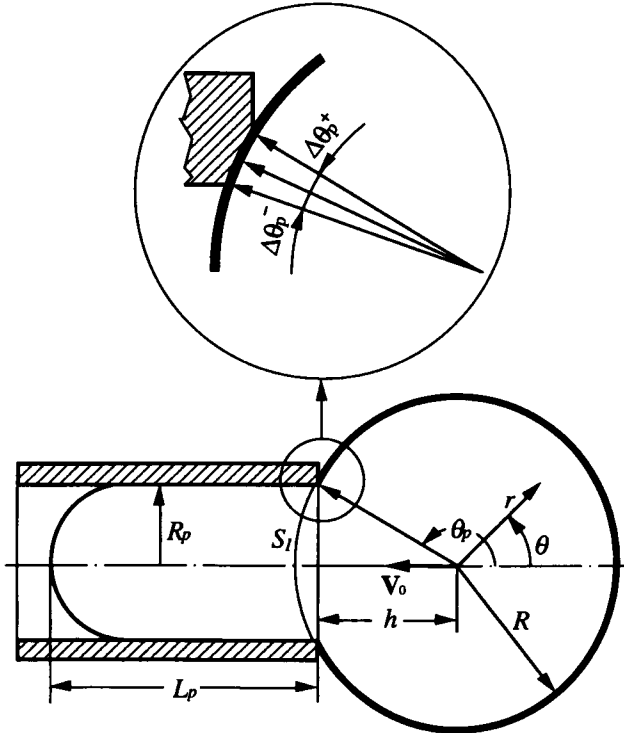where $\sigma_{r\theta}$ and σ_{rr} are shear and normal stresses on the

FIGURE 2 Schematics and geometry for the analysis of a single cell entering a micropipette at a fixed aspiration pressure.

boundary, respectively, R is the instantaneous cell radius, R_f is the radius of the cell projection inside the pipette, p_a is the ambient pressure, p_p is the suction pressure inside the pipette, T is the cortical tension, $\zeta_p = \cos \theta_p$, $\epsilon = \zeta_p - \cos(\theta_p + \Delta\theta_p^-) = \cos(\theta_p - \Delta\theta_p^+) - \zeta_p$, and k is a uniform reaction stress from the pipette in the finite contact area between the cell and the pipette (cf. Fig. 2). In our simulation, the value of ϵ was set to 0.1, which represented a contact area close to what we observed in our experiments. It should also be pointed out that the cytoplasmic flow is not particularly sensitive to ϵ when tested in a range from 0 to 0.20 in our numerical simulation.

For a Newtonian fluid, the constitutive relations between the stress components and flow field are governed by

$$\sigma_{rr} = -p + 2\mu \frac{\partial V_r}{\partial r}, \tag{11}$$

$$\sigma_{r\theta} = \mu \left[\frac{1}{r} \frac{\partial V_r}{\partial \theta} + r \frac{\partial}{\partial r}\left(\frac{V_\theta}{r}\right) \right]. \tag{12}$$

By applying the boundary conditions, the cytoplasmic flow field was determined as

$$V_r = -V_0 \zeta \tag{13}$$

$$+ \frac{\Delta pR}{4\mu} \sum_{n=3}^{\infty} \left[n\left(\frac{r}{R}\right)^n - \frac{n^2 - 1}{n - 2}\left(\frac{r}{R}\right)^{n-2} \right] f_n(\zeta_p, \epsilon) P_{n-1}(\zeta),$$

$$V_\theta = V_0 \sin \theta - \frac{\Delta pR}{4\mu} \tag{14}$$

$$\cdot \sum_{n=3}^{\infty} n\left[(n + 2)\left(\frac{r}{R}\right)^n - \frac{n^2 - 1}{n - 2}\left(\frac{r}{R}\right)^{n-2} \right] f_n(\zeta_p, \epsilon) \frac{I_n(\zeta)}{\sin \theta},$$

where V_0 is the center velocity of the spherical body outside the pipette and is determined by the constraint that the cell cortical membrane keeps contacting with the tip of the micropipette:

$$V_0 = -\frac{\Delta pR}{4\mu} \tag{15}$$

$$\cdot \sum_{n=3}^{\infty} f_n(\zeta_p, \epsilon)\left[\frac{2n - 1}{n - 2} \zeta_p P_{n-1}(\zeta_p) + \frac{3n}{n - 2} I_n(\zeta_p) \right].$$

Other notations were defined as

$$f_n(\zeta_p, \epsilon) = \frac{(2n - 1)(n - 1)}{2n^2 + 1}$$

$$\cdot \left[\left(\frac{1}{2} - \frac{1 - \zeta_p^2 - \epsilon^2}{4\zeta_p \epsilon}\right) I_n(\zeta_p - \epsilon) \right. \tag{16}$$

$$\left. + \left(\frac{1}{2} + \frac{1 - \zeta_p^2 - \epsilon^2}{4\zeta_p \epsilon}\right) I_n(\zeta_p + \epsilon) \right],$$

$$\Delta p = \Delta p_h\left[1 - \beta\left(\frac{R_p}{R_f} - \frac{R_p}{R}\right) \right]. \tag{17}$$

In Eq. 17, Δp_h is a hydrostatic aspiration pressure,

$$\Delta p_h = p_a - p_p. \tag{18}$$

R_p is the pipette radius, and β, proportional to the ratio of the threshold pressure to the hydrostatic aspiration pressure, is defined as

$$\beta = \frac{2T}{R_p} \bigg/ \Delta p_h. \tag{19}$$

Shear rate definitions

The rate of viscous energy dissipation is proportional to ϕ:

$$\phi = \tfrac{1}{2}\epsilon_{ij}\epsilon_{ij} \qquad i,j = 1, 2, 3, \tag{20}$$

where ϵ_{ij} are components of the cellular deformation rate tensor and the indices 1, 2, and 3 refer to the r, θ, and φ directions, respectively. The shear rate, a function of position within the cell and time, was therefore defined as

$$\dot{\gamma} = \sqrt{\phi}. \tag{21}$$

An instantaneous mean shear rate, $\dot{\gamma}_a$, was defined as an average of ϕ over the spherical portion of the cell volume (cf. Appendix), and a mean shear rate, $\dot{\gamma}_m$, was defined as an average of ϕ over the spherical cell volume and throughout the whole aspiration process,

$$\dot{\gamma}_a = \left(\frac{3}{2} \int_0^{R(t)} \int_0^{\pi} \frac{r^2}{R^3} \phi \sin \theta \, d\theta \, dr \right)^{1/2}, \tag{22a}$$

$$\dot{\gamma}_m = \left(\frac{3}{2} \frac{1}{t_e} \int_0^{t_e} \int_0^{R(t)} \int_0^{\pi} \frac{r^2}{R^3} \phi \sin \theta \, d\theta \, dr \, dt \right)^{1/2}. \tag{22b}$$

Physically, the mean shear rates defined above are indicators of an average viscous energy dissipation at an instant during the cell entry or averaged over the entire process. For a uniform steady shear flow, $\dot{\gamma}_a$ and $\dot{\gamma}_m$ take the true value of shear rate.

Simulation results of Newtonian liquid drop

In solving the cell entry problem, the solution to the cytoplasmic flow in the spherical cell body outside the micropipette was calculated numerically at each incremental time step until the whole cell entered the micropipette, that is, $R/R_p = 1$. Computations do not converge fast enough to control the accumulated error of the computation at the contact region between the cell and the micropipette. Thus, the technique of polynomial extrapolation was employed to approximate those values (Press et al., 1989).

As shown in Fig. 3, for a given value of β ($0 \leq \beta \leq 0.20$), cell entry time, t_e, is a function of the ratio of initial cell radius
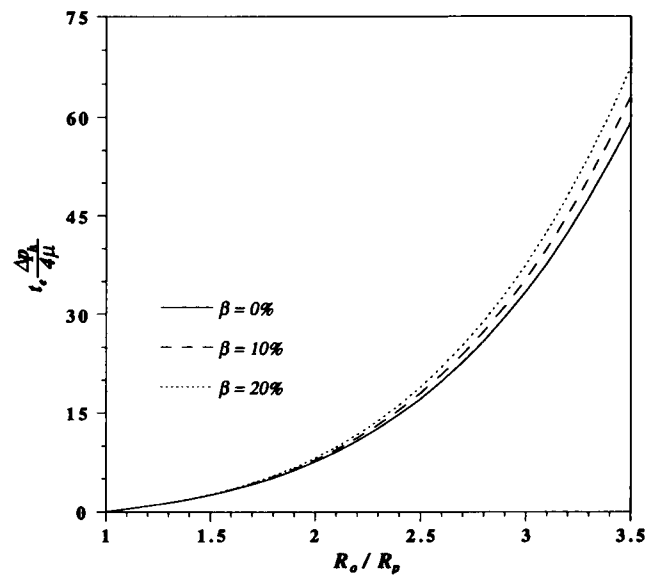

FIGURE 3   Entry time for whole cell aspiration as a function of initial cell size, R_0/R_p, for three different ratios of the threshold pressure to the hydraulic aspiration pressure, β.

to the pipette size, R_0/R_p, and can be approximated as

$$t_e = \frac{4\mu}{\Delta p_h} \left[a_0 + a_1 \left(\frac{R_0}{R_p} \right) + a_2 \left(\frac{R_0}{R_p} \right)^2 + a_3 \left(\frac{R_0}{R_p} \right)^3 \right]$$

$$\cdot \sqrt{\left(\frac{R_0}{R_p} \right)^2 - 1}, \tag{23}$$

where coefficients a_i ($i = 0, 1, 2, 3$) are β dependent and were determined with least-squares fits as

$$a_0 = -1.3079 - 0.019975\beta$$
$$+ 0.13869\beta^2 - 0.87898\beta^3, \tag{24}$$

$$a_1 = 2.0756 - 0.21461\beta$$
$$+ 0.065414\beta^2 + 2.0469\beta^3, \tag{25}$$

$$a_2 = -0.37513 - 0.10393\beta$$
$$- 0.4992\beta^2 - 1.6295\beta^3, \tag{26}$$

$$a_3 = 0.38012 + 0.29926\beta$$
$$+ 0.28995\beta^2 + 0.45455\beta^3. \tag{27}$$

The degree of polynomials in β was chosen to ensure an accuracy of 0.01% to the numerical results.

Thus, the apparent cytoplasmic viscosity, μ, can be assessed from whole cell aspiration experiments by

$$\mu = \frac{\Delta p_h \cdot t_e}{4 \left[a_0 + a_1 \left(\frac{R_0}{R_p} \right) + a_2 \left(\frac{R_0}{R_p} \right)^2 + a_3 \left(\frac{R_0}{R_p} \right)^3 \right] \sqrt{\left(\frac{R_0}{R_p} \right)^2 - 1}} \tag{28}$$

as the cell entry time, t_e, cell size, R_0/R_p, and hydraulic suction pressure Δp_h can be measured directly from the whole

FIGURE 4 Instantaneous shear rate distribution. $(a) R/R_p = 2.3$; $(b) R/R_p = 1.9$; $(c) R/R_p = 1.5$; $(d) R/R_p = 1.1$. The black regions represent the highest values of shear rate and the light gray represents the lowest values. The shear rate mainly concentrates in the vicinity of the contact area between the cell and the pipette tip and propagates to a larger fraction of the sperical volume as the aspiration process progresses.
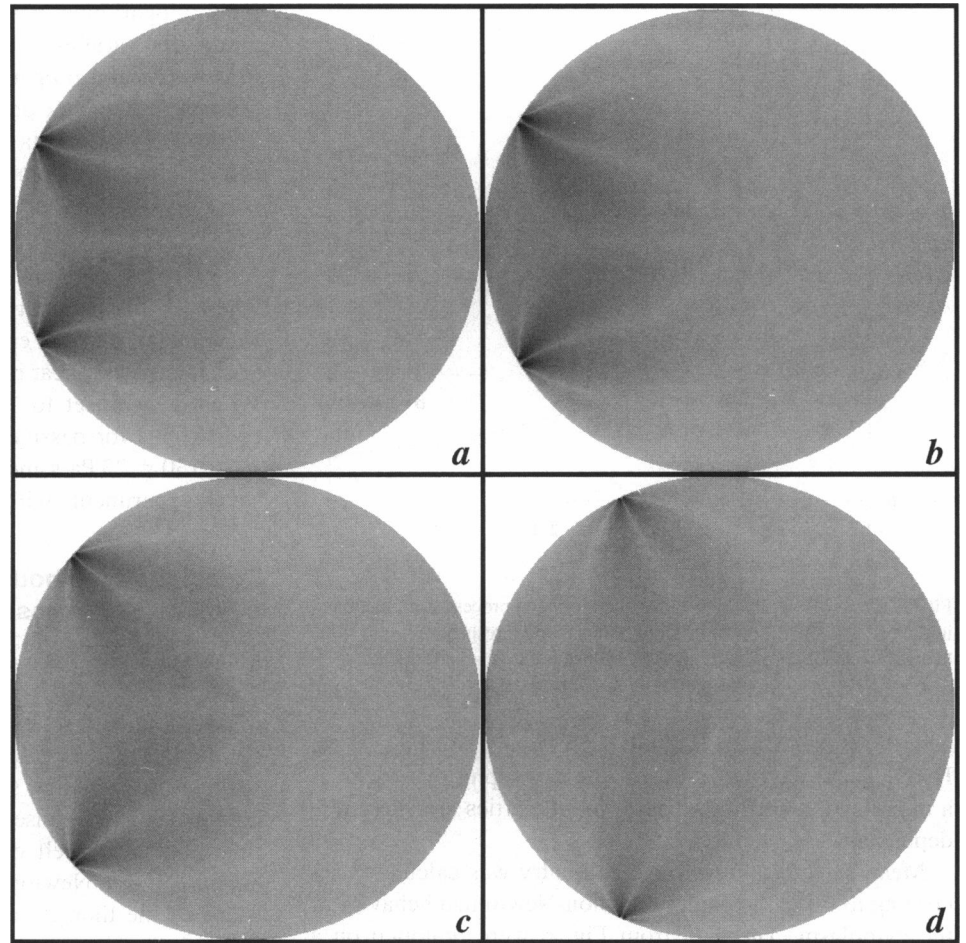
cell aspiration experiments and the ratio of the threshold pressure to the hydraulic aspiration pressure, β, can be determined from the measured cortical tension.

Four instantaneous shear rate distributions are shown in Fig. 4 for a "cell" entering a micropipette. The black regions represent the highest shear rate and the light gray represents the lowest shear rate, which is close to zero. The calculations indicate that most of the viscous energy dissipation is concentrated in the vicinity of the contact area between the cell and the pipette. They also indicate that the propagation of high shear rate is constrained within the sphere. That is, the viscous energy dissipation outside the sphere is very small in comparison with that within the sphere. This is consistent with the experimental observation that the cytoplasmic flow inside the micropipette is nearly a "plug flow."

The mean shear rate for the whole cell aspiration process was determined as a function of the initial cell size, pipette size, and cell cortical tension (Fig. 5). Note that the influence of the cortical tension is very slight. This function can be approximated by

$$\dot{\gamma}_m = \frac{\Delta p_h}{4\mu} \frac{b_0 + b_1(R_0/R_p) + b_2(R_0/R_p)^2 + b_3(R_0/R_p)^3}{[(R_0/R_p)^2 - 1]^{7/20}} \qquad (29)$$

where b_i ($i = 0, 1, 2, 3$) are functions of β, given approxi-

mately (to an accuracy of 0.01%) as

$$b_0 = 8.8685 + 1.8690\beta, \qquad (30)$$

$$b_1 = -4.4846 - 2.7003\beta, \qquad (31)$$

$$b_2 = 1.0322 + 0.9222\beta, \qquad (32)$$

$$b_3 = -0.09117 - 0.1027\beta. \qquad (33)$$

Thus, the mean shear rate, $\dot{\gamma}_m$, can be estimated for a single cell entering a micropipette.

RESULTS AND DISCUSSION

Neutrophil cytoplasmic viscosity

The apparent cytoplasmic viscosity of the neutrophil was calculated with Eq. 28 from measurements of whole cell aspiration times. A total of 835 cells were measured at aspiration pressures ranging from 98 to 882 Pa, using pipettes from 4.0 to 5.0 μm in diameter. Results from a typical experiment are shown in Fig. 6 for whole cell aspirations into a 4.0-μm-diameter pipette. As evidenced in Fig. 6, neutrophil cytoplasmic viscosity is a function of aspiration pressure, or more precisely, it is shear rate dependent. The value of the viscosity ranges from ~500 Pa·s at an aspiration pres-
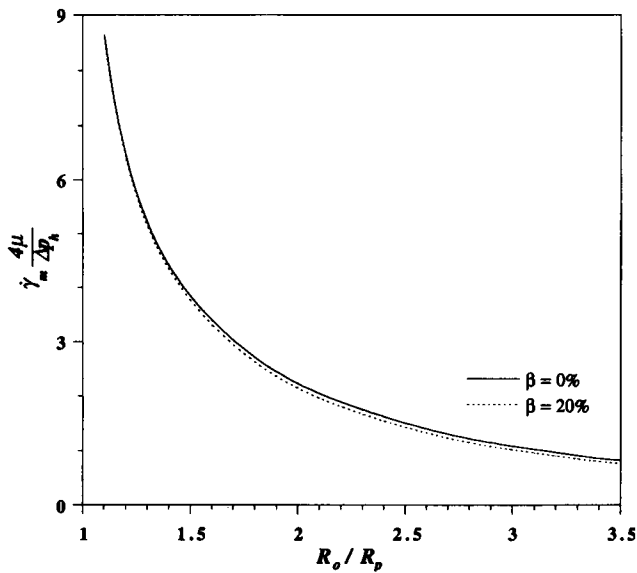
FIGURE 5   Mean shear rate during the aspiration process as a function of initial cell size, R_o/R_p, under different ratios of the threshold pressure to the hydraulic aspiration pressure, β. The influence by β is very slight.

sure of 98 Pa (1.0 cm H_2O) to ~55 Pa·s at 882 Pa (9.0 cm H_2O). These data indicate that the neutrophil cytoplasm is a non-Newtonian fluid, that is, its properties are shear rate dependent.

Mean shear rate during the cell entry was calculated according to Eq. 29 to explore the non-Newtonian behavior of the cytoplasm. The data from Fig. 6 were replotted on a natural logarithmic scale (Fig. 7). Error bars indicate the SDs

for the logarithms of viscosity and shear rate within each group. The variability in shear rate resulted from differences in cell size and properties as all cells in each group were aspirated at the same pressure. The linear relationship in Fig. 7 ($r > 0.95$) suggests that the mechanical behavior of the neutrophil can be approximated as a power-law fluid:

$$\mu = \mu_c \left(\frac{\dot{\gamma}_m}{\dot{\gamma}_c}\right)^{-b} \qquad (34)$$

where μ is the apparent cytoplasmic viscosity, $\dot{\gamma}_m$ is the mean shear rate during cell entry, μ_c is the characteristic viscosity at characteristic shear rate $\dot{\gamma}_c$, and b is a material coefficient. When $\dot{\gamma}_c$ was set to 1 s^{-1} for convenience, the material coefficients for passive neutrophils were determined to be $\mu_c = 130 \pm 23$ Pa·s and $b = 0.52 \pm 0.09$ based on data from seven experiments with a total number of 835 cells.

Calculation methods and discrepancies in cytoplasmic viscosity

Shown in Table 1 is a comparison of values of cytoplasmic viscosity calculated by three different methods from the data of one complete series of aspiration pressures. In the first column are values calculated from the total entry time, as outlined in preceding sections of this paper. In the second column are values based on a least-squares regression to the time course for cell entry calculated from the numerical simulation of a Newtonian drop. It should be noted that the shape of the time course for cell entry predicted from the
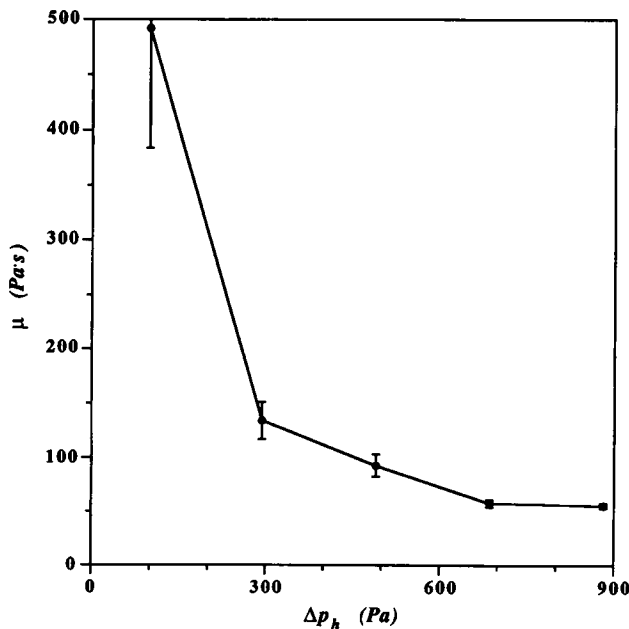

FIGURE 6   Apparent cytoplasmic viscosity determined at aspiration pressures ranging from 98 to 882 Pa for normal neutrophils. Viscosity was calculated from whole cell aspiration times with a pipette diameter of 4.0 μm. Each point represents the mean value for measurements on 10–15 cells. The vertical bars represent SEs.
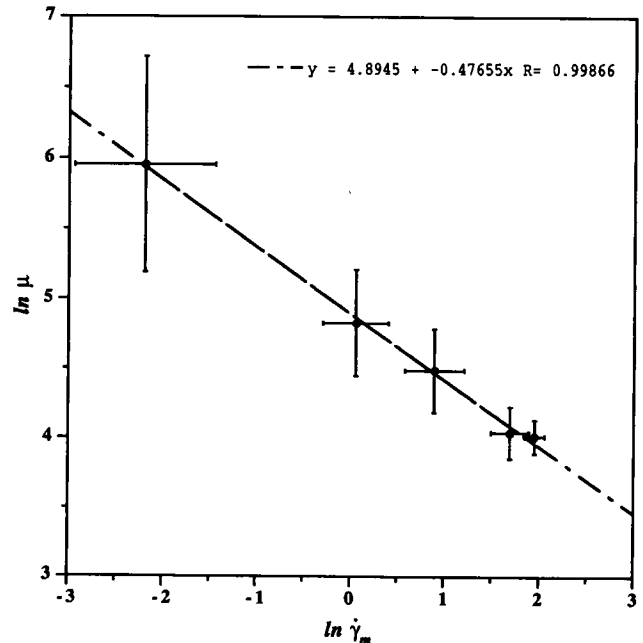

FIGURE 7   The cytoplasmic viscosity as a function of mean shear rate in logarithmic scale calculated from a whole cell aspiration experiment with a pipette diameter of 4.0 μm. Each point represents the mean of 10–15 cells at a given aspiration pressure, where the horizontal and vertical bars indicate the SDs. The straight line is a least-square fit to the means with correlation coefficient >0.99.

TABLE 1　Neutrophil cytoplasmic viscosity calculated by three different methods (see Fig. 8)

Δp (cm H_2O)	μ (Pa·s)		
	Cell entry time	Least-squares fit	N-H method
1.0	492 ± 108	450 ± 93	1348 ± 318
3.0	134 ± 17	137 ± 13	349 ± 50
5.0	92 ± 9	97 ± 7	231 ± 14
7.0	58 ± 3	58 ± 4	160 ± 15
9.0	56 ± 2	58 ± 2	154 ± 6
μ_c (Pa·s)	133	134	223
b	0.48	0.47	0.47

The calculations indicate that neutrophil cytoplasm exhibits shear thinning no matter which method is used to calculate the viscosity. Material coefficients μ_c and b were obtained by least-squares regression for the characteristic shear rate, $\dot{\gamma}_c$, set to 1 s^{-1}. Note that all three methods produce essentially the same value for the parameter b.

Newtonian model did not agree precisely with the observed cell entry as shown in Fig. 8. The real cell generally entered more rapidly at first, more slowly during the "middle" period, and more rapidly at the end. This has been recognized by other investigators and prompted Needham and Hochmuth (1990) to devise an alternative method for calculating the cytoplasmic viscosity. In this method, cell entry rate, dL_p/dt, was measured at the point when half the cell volume was aspirated into the micropipette, and the apparent viscosity was calculated by

$$\mu = \frac{\Delta p \cdot R_p R}{m(R - R_p)dL_p/dt} \tag{35}$$

where R is the instantaneous cell radius and m is a parameter accounting for the effect of energy dissipation within the cortical membrane. According to Evans and Yeung (1989), $m = 6$. Values calculated by this approach are shown in column 3. The two methods based on the current analysis, least-squares regression to the predicted time course or calculation based on total cell entry time, yield very similar values. The method used by Needham and Hochmuth produces values that are significantly larger. Two points need to be emphasized. First, the shear rate dependence of the viscosity, reflected by the parameter b (cf. Table 1), is essentially the same for all three methods. This confirms that the viscosity is shear rate dependent and that this dependence is *not* an artifact of the method used to calculate the viscosity. Second, the Needham-Hochmuth method confines itself to the time at which the rate of cell entry is the slowest. Thus, the differences in the values obtained by the different methods appear to reflect the shear rate or range of shear rates over which the calculation was made.

Power-law fluid: a promising candidate for the neutrophil mechanical model

The present data show clearly that the mechanical behavior of neutrophil cytoplasm is non-Newtonian. This behavior can be further characterized as that of a power-law fluid. This
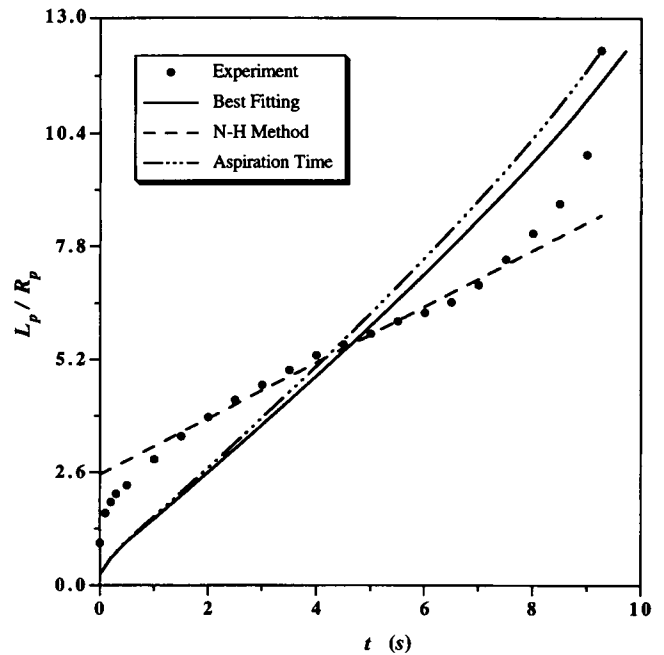

FIGURE 8　Time course of a neutrophil entering a 4.0-μm micropipette at an aspiration pressure of 490 Pa in comparison with the results of numerical simulation. ●, experimental data points; ———, least-squares fit; — — — —, curve fit with a cytoplasmic viscosity calculated according to the method of Hochmuth and Needham (1990); — · · · —, curve fit with the cytoplasmic viscosity calculated via whole cell aspiration time. It is evident that significant discrepancies exist between the experiment results and theoretical predictions.

model is an appropriate description for most particulate and polymeric liquids over a remarkable range of shear rate (Bird et al., 1987). In particular, the power-law approximation is a good description of the rheological properties of F-actin solutions in vitro. F-actin is known to play the major role in neutrophil motility and is believed to be the major determinant of the passive mechanical properties of the cell (Stossel, 1984, 1988). In vitro rheological studies indicate that a solution of filamentous actin behaves generally as a power-law fluid with an exponent of 0.7 to 0.8, a somewhat stronger dependence than what is observed for the cytosol (Zaner and Stossel, 1982; Oppermann and Jaberg, 1985). Two factors may contribute to the higher exponent for actin solutions compared to cytosol. First, although the total concentrations of actin in those experiments were similar to the concentration in neutrophils, the concentration of F-actin in the experimental solutions was much higher than in the neutrophil cytoplasm, because 70–80% of neutrophil actin is in monomeric form in situ (Sheterline and Rickard, 1989). Second, the chain length of F-actin filaments in the solutions was greater than that in the neutrophil cytoplasm (Hartwig et al., 1985, 1988). The shear rate dependence of viscosity is known to increase with increasing polymer concentration and filament length.

Most interestingly, the power-law approximation enables us to reconcile diverse values of cytoplasmic viscosity obtained in different laboratories with different techniques

TABLE 2 Comparison of the power-law fluid prediction with published values of cytoplasmic viscosity

Authors	$\dot{\gamma}_m$	μ (Pa·s)	Prediction*
Needham and Hochmuth, 1990	1.27–14.40‡	135	41–140
Evans and Yeung, 1989	0.69–2.11‡	210	76–240
Valberg and Albertini, 1985	0.003§	2400¶	1800–7900 (2700)ǁ
Valberg and Albertini, 1985	0.001§	4400¶	2900–15,400 (4700)ǁ

* Calculated from mean ± SD of the material constants.

‡ Values were obtained according to the present numerical analysis based on the reported values of respective initial cell diameters, aspiration pressures and cytoplasmic viscosity.

§ Reported values by Valberg and Albertini, which were calculated based on Stokes flow around a solid sphere (Valberg and Albertini, 1985).

¶ The value was adjusted for temperature according to Evans and Yeung (Evans and Yeung, 1989).

ǁ Calculation by using mean values of material constants for the power-law behavior.

(Valberg and Albertini, 1985; Zaner and Valberg, 1989; Evans and Yeung, 1989; Needham and Hochmuth, 1990) as shown in Table 2. In particular, and in contrast to other current mechanical models, the power-law fluid model is in excellent agreement with the measurements by magnetic probes inside living cells (Valberg and Albertini, 1985), even though the values are one to two orders of magnitude higher than those obtained by micropipette aspiration techniques (Evans and Yeung, 1989; Needham and Hochmuth, 1990). Thus, the power-law fluid appears to be an appropriate model for the passive mechanical behavior of human neutrophils over a broad range of shear rates.

In addition to reconciling results obtained from different laboratories, shear thinning can also account for some discrepancies between details of cellular behavior in micromechanical experiments and predictions of cellular behavior based on a purely Newtonian fluid model. For example, observations of the cell recovering its spherical shape after expulsion from the micropipette (Tsai, 1992) indicate that the initial recovery is more rapid and the late stage of recovery more gradual than what is predicted by an analysis based on a Newtonian liquid drop (Tran-Son-Tay et al., 1991). When the cell is first released from a micropipette, a large driving force originating from the cortical tension and a large curvature generates a flow field with a high shear rate. The high shear rate causes a low cytoplasmic viscosity, and thus low viscosity could account for a high initial rate of recovery. Subsequently, the recovery rate, or the shear rate, decreases with the driving force as the process progresses. The decreased shear rate results in higher cytoplasmic viscosity, further reducing the recovery speed. This would account for the disparity between the prediction of the Newtonian liquid drop model (Tran-Son-Tay et al., 1991) and experimental observation for the time course of the cell recovery (Tsai, 1992).

In the case of cell entry into a micropipette, it is commonly observed that the cell enters the pipette more rapidly than predicted when aspiration is nearly complete. This is most likely attributable to shear thinning. A gradual increase in shear rate occurs during the course of the whole cell aspiration and so would be expected to lead to a decrease in apparent viscosity with the progression of cell entry. The decreased viscosity would lead to a further increase in entry rate, and thus a positive feedback is established between shear rate and viscosity. This positive feedback could account for the rapid entry rate observed at the final phase of the cell aspiration process. To assess this possibility the time course of cell entry was calculated under the assumption that the cytoplasm has a uniform instantaneous viscosity at each time step and the instantaneous viscosity has a power-law relationship to the instantaneous shear rate averaged over the cell volume (see Appendix for details). Fig. 9 shows the numerical prediction in comparison with the time course of a neutrophil entering a 4.0-μm micropipette under an aspiration pressure of 490 Pa. The parameters μ_o (defined in the Appendix) and b were obtained by a least-squares regression to the experimental data. For this particular fit, $b = 0.73$ and $\mu_o = 6.4$ Pa·s or $\mu_c = 55$ Pa·s when $\dot{\gamma}_c = 1$ s^{-1}. Generally, the parameter b was larger when determined by this approach for individual cells than when determined from calculations based on the entry time of cells at different aspiration pressures. This is probably due to the different assumptions and approximations of shear rate used in the different methods.

It should be noted that the initial, rapid phase of cell entry is not predicted using this approach and that an arbitrary
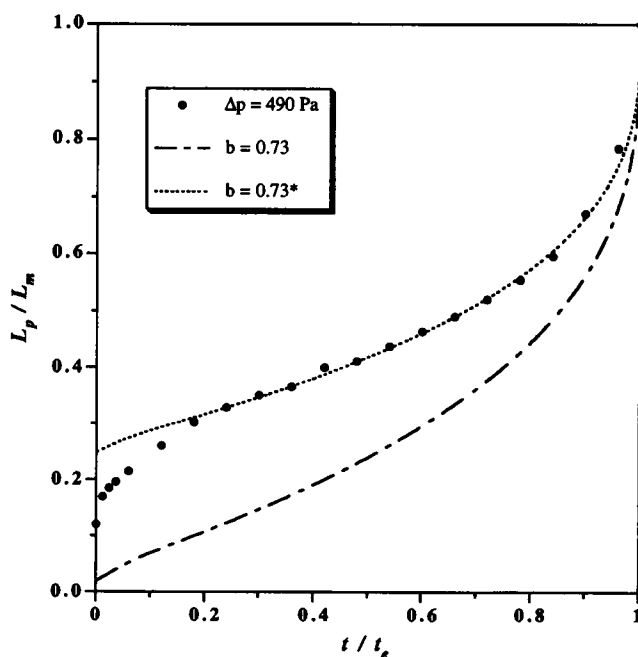

FIGURE 9 Numerical prediction of a homogeneous power-law fluid with $b = 0.73$ in comparison with the time course of a neutrophil entering a 4.0-μm pipette at an aspiration pressure of 490 Pa. ●, experimental data points; ———, numerical prediction for the homogeneous fluid without allowing a spontaneous initial projection; ········, numerical prediction obtained by introducing an arbitrary initial cell projection length. The reference viscosity μ_o was determined to be 6.4 Pa·s, and the characteristic viscosity, μ_c, was ~55 Pa·s.

initial projection length was introduced to obtain the match shown in the figure. The rapid deformation of neutrophils at small deformations has been treated recently in an article by Hochmuth and co-workers (Hochmuth et al., 1993), who argue that the cytoplasmic viscosity is small when cellular deformation is small. That work is complementary to the present analysis, which applies to large cytoplasmic deformations at different shear rates.

As a final note, we should emphasize that a true numerical simulation of the entry of a power-law cytosol into a micropipette has not been completed. Such an analysis is complicated by the fact that the shear rate, and therefore the cytoplasmic viscosity, varies both spatially and in time. In obtaining the curve fits shown in Fig. 9, we accounted only for the temporal dependence and ignored spatial variations in shear rate within the cytosol. Even so, this simplified model required significant supercomputing time to develop. While it is clear that a complete power-law fluid analysis is desirable, it is a task too large to be included in the present work. Our goal here is simply to document that the phenomenon exists and to illustrate how it can account for certain discrepancies that have been noted for the simpler Newtonian liquid drop model.

CONCLUSION

The findings of the present study are consistent with previous work in other laboratories (Evans and Kukan, 1984; Evans and Yeung, 1989; Hochmuth and Needham, 1990; Needham and Hochmuth, 1990) but provide new insights into neutrophil mechanical properties. Methods for calculating the cytoplasmic viscosity (cf. Eq. 28) and mean shear rate (cf. Eq. 29) combined with the micropipette aspiration experiments provide a simple approach to investigating the mechanical properties of human neutrophils at the cellular level. Consistent with previous studies, the apparent viscosity of neutrophil cytoplasm ranged from 500 Pa·s at an aspiration pressure of 98 Pa to 50 Pa·s at 882 Pa when tested with a 4.0-μm pipette. Most importantly, the current study elucidates the fact that neutrophil cytoplasm exhibits shear thinning behavior, indicating that a power-law fluid model is a more appropriate description of the neutrophil cytoplasm.

APPENDIX

The validity of the power-law fluid model is examined in this Appendix by simply assuming that the neutrophil cytoplasm is a homogeneous fluid, but the viscosity varies with the instantaneous mean shear rate averaged over the cell volume. The relationship between viscosity and shear rate is assumed to follow a power-law function:

$$\mu = \mu_0 \left(\frac{\dot{\gamma}_a}{\dot{\gamma}_0} \right)^{-b} \tag{A1}$$

where $\dot{\gamma}_a$ is the mean shear rate average over the spherical portion of cell volume outside the micropipette, $\dot{\gamma}_0$ is a reference shear rate, and μ_0 is a reference viscosity when $\dot{\gamma}_a = \dot{\gamma}_0$. Note that μ_0 is not the same as μ_c given in Table 1. For convenience, $\dot{\gamma}_0$ is defined as

$$\dot{\gamma}_0 = \frac{\Delta p_h}{4\mu_0}. \tag{A2}$$

The components of the deformation rate tensor are designated as

$$\epsilon_{ij} = \frac{\Delta p_h}{4\mu} \left[1 - \beta \left(\frac{R_p}{R_f} - \frac{R_p}{R} \right) \right] \hat{e}_{ij} \tag{A3}$$

where $\hat{e}_{ij}$ are determined from Eqs. 13–15 as

$$\hat{e}_{r\varphi} = 0 \tag{A4}$$

$$\hat{e}_{\theta\varphi} = 0, \tag{A5}$$

$$\hat{e}_{rr} = \sum_{n=3}^{\infty} \left[n^2 \left(\frac{r}{R} \right)^2 - (n^2 - 1) \right] \left(\frac{r}{R} \right)^{n-3} f_n(\zeta_p, \epsilon) P_{n-1}(\zeta), \tag{A6}$$

$$\hat{e}_{r\theta} = \left[1 - \left(\frac{r}{R} \right)^2 \right] \sum_{n=3}^{\infty} n^2(n^2 - 1) \left(\frac{r}{R} \right)^{n-3} f_n(\zeta_p, \epsilon) \frac{I_n(\zeta)}{\sin\theta}, \tag{A7}$$

$$\hat{e}_{\theta\theta} = \left\{ -\sum_{n=3}^{\infty} (n + 1) \left[n \left(\frac{r}{R} \right)^2 - \frac{(n - 1)^2}{n - 2} \right] \left(\frac{r}{R} \right)^{n-3} f_n(\zeta_p, \epsilon) P_{n-1}(\zeta) \right.$$
$$\left. + \frac{\zeta}{1 - \zeta^2} \sum_{n=3}^{\infty} n \left[(n + 2) \left(\frac{r}{R} \right)^2 - \frac{(n - 1)^2}{n - 2} \right] \left(\frac{r}{R} \right)^{n-3} f_n(\zeta_p, \epsilon) I_n(\zeta) \right\}, \tag{A8}$$

$$\hat{e}_{\varphi\varphi} = \left\{ \sum_{n=3}^{\infty} \left[n \left(\frac{r}{R} \right)^2 - \frac{(n - 1)^2}{n - 2} \right] \left(\frac{r}{R} \right)^{n-3} f_n(\zeta_p, \epsilon) P_{n-1}(\zeta) \right.$$
$$\left. - \frac{\zeta}{1 - \zeta^2} \sum_{n=3}^{\infty} n \left[(n + 2) \left(\frac{r}{R} \right)^2 - \frac{(n - 1)^2}{n - 2} \right] \left(\frac{r}{R} \right)^{n-3} f_n(\zeta_p, \epsilon) I_n(\zeta) \right\}. \tag{A9}$$

The instantaneous average shear rate is defined as (cf. Eq. 22a)

$$\dot{\gamma}_a = \left[\frac{3}{2} \int_0^R \frac{r^2}{R^3} \int_0^\pi \left(\frac{1}{2} \epsilon_{ij}\epsilon_{ij} \right) \sin\theta \, d\theta \, dr \right]^{1/2} \tag{A10}$$

and can be determined by substituting Eqs. A1 and A2 into the above equation:

$$\frac{\dot{\gamma}_a}{\dot{\gamma}_0} = \left\{ \left[1 - \beta \left(\frac{R_p}{R_f} - \frac{R_p}{R} \right) \right] \Phi \right\}^{1/(1-b)} \tag{A11}$$

where the function Φ is designated as

$$\Phi = \left[\frac{3}{4} \int_0^R \frac{r^2}{R^3} \int_0^\pi (\hat{e}_{rr}^2 + \hat{e}_{r\theta}^2 + \hat{e}_{\theta\theta}^2 + \hat{e}_{\varphi\varphi}^2) \sin\theta \, d\theta \, dr \right]^{1/2}. \tag{A12}$$

Hence, the instantaneous shear rate averaged over cell volume can be determined for a given cell radius.

From Eqs. 13 and 14, the flow rate into the micropipette can be determined as

$$Q = \frac{\pi R_p^3 \cdot \Delta p_h}{4\mu_0} \left(\frac{\dot{\gamma}_a}{\dot{\gamma}_0} \right)^b \left[1 - \beta \left(\frac{R_p}{R_f} - \frac{R_p}{R} \right) \right] \hat{q}, \tag{A13}$$

where

$$\hat{q} = R \left\{ \sum_{n=3}^{\infty} \frac{2n - 1}{n - 2} \left(\frac{r}{R} \right)^{n-2} f_n(\zeta_p, \epsilon)[2\bar{R}^2 I_n(\zeta_p) - \zeta_p P_{n-1}(\zeta_p)] \right.$$
$$\left. - 3 \sum_{n=3}^{\infty} \frac{n}{n - 2} \left(\frac{r}{R} \right)^{n-2} f_n(\zeta_p, \epsilon) I_n(\zeta_p) \right\}, \qquad \frac{r}{R} \to 1 \tag{A14}$$

and $\bar{R} = R/R_p$. Polynomial extrapolation is used to determine $\hat{q}$ because the series converges very slowly with n.

From the conservation of cell volume, cell entry rate, dL_p/dt, is determined by

$$\frac{dL_p}{dt} = \frac{G}{\pi R_p^2} Q, \tag{A15}$$

that is,

$$\frac{d\bar{L}_p}{d\bar{t}} = G \left(\frac{\dot{\gamma}_a}{\dot{\gamma}_o}\right)^b \left[1 - \beta\left(\frac{1}{\bar{R}_f} - \frac{1}{\bar{R}}\right)\right] \hat{q}, \tag{A16}$$

where G is a geometrical factor:

$$G = \begin{cases} 2/(1 + \bar{L}_p^2) & \bar{L}_p \leq 1 \\ 1 & \bar{L}_p > 1 \end{cases} \tag{A17}$$

and the nondimensionalized variables in Eqs. A15-A17 are defined as

$$\bar{R}_f = \frac{R_f}{R_p}, \qquad \bar{L}_p = \frac{L_p}{R_p}, \qquad \bar{t} = t \bigg/ \sqrt{\frac{4\mu_o}{\Delta p_h}}.$$

Based on Eqs. A11, A14, and A16, cell projection length can be determined as a function of the dimensionless time for a given material coefficient b and initial cell radius R_0/R_p. Shown in Fig. 9 are the numerical simulation results in comparison with experimental data. An initial projection length L_0 was introduced to account for the initial rapid entry of the cell into the micropipette. Thus, the starting value for the cell radius R_0 was slightly smaller than the spherical cell radius. The material parameter, b, was manually adjusted in steps of 0.01 to obtain the best visual agreement between the theoretical prediction and experimental data. The theoretical prediction was expressed in terms of the normalized time ratio, $\bar{t}/\bar{t}_e$, which is equal to the real time ratio, t/t_e. The parameter μ_o was obtained by equating

$$t_e = \frac{4\mu_o}{\Delta p_h} \bar{t}_e. \tag{A18}$$

The results in Fig. 9 show clearly that the power-law fluid model has the capability to account for discrepancies in the details of cellular behavior observed in experiments and those of theoretical predictions based on the other current models.

REFERENCES

Bainton, D. F. 1988. Phagocytic cells: developmental biology of neutrophils and eosinophils. In Inflammation: Basic Principles and Clinical Correlates. J. I. Gallin, I. M. Goldstein, and R. Snyderman, editors. Raven Press, New York. 265–280.

Bird, R. B., R. C. Armstrong, and O. Hassager. 1987. Dynamics of Polymeric Liquids. Vol. 1. Fluid Mechanics. John Wiley and Sons, New York.

Chien, S., and P-L. P. Sung. 1984. Effect of colchicine on viscoelastic properties of neutrophils. Biophys. J. 46:383–386.

Dong, C., R. Skalak, K-L. P. Sung, G. W. Schmid-Schönbein, and S. Chien. 1988. Passive deformation analysis of human leukocytes. J. Biomech. Eng. 110:27–36.

Dong, C., R. Skalak, and K-L. P. Sung. 1991. Cytoplasmic rheology of passive neutrophils. Biorheology. 28:557–567.

Evans, E., and B. Kukan. 1984. Passive material behavior of granulocytes based on large deformation and recovery after deformation tests. Blood. 64:1028–1035.

Evans, E., and A. Yeung. 1989. Apparent viscosity and cortical tension of blood granulocytes determined by micropipet aspiration. Biophys. J. 56: 151–160.

Frank, R. S., and M. A. Tsai. 1990. The behavior of human neutrophils during flow through capillary pores. J. Biomech. Eng. 112:277–282.

Happel, J., and H. Brenner. 1983. Low Reynolds Number Hydrodynamics. Martinus Nijhoff Publishers, Boston, MA.

Hartwig, J. H., R. Niederman, and S. E. Lind. 1985. Cortical actin structure and their relationship to mammalian cell movements. Subcell. Biochem. 11:1–49.

Hartwig, J. H., K. S. Zaner, and P. A. Janmey. 1988. The cortical actin gel of macrophages. In Cell Physiology of Blood. R. B. Gunn and J. C. Parker, editors. Rockefeller University Press, New York. 125–140.

Hochmuth, R. M., and D. Needham. 1990. The viscosity of neutrophils and their transit times through small pores. Biorheology. 27:817–828.

Hochmuth, R. M., H. P. Ting-Beall, B. B. Beaty, D. Needham, and R. Tran-Son-Tay. 1993. Viscosity of passive human neutrophils undergoing small deformations. Biophys. J. 64:1596–1601.

Janmey, P. A. 1991. Mechanical properties of cytoskeletal polymers. Curr. Opin. Cell Biol. 2:4–11.

Lamb, H. 1945. Hydrodynamics. Dover Publications, New York.

Lichtman, M. A., and E. A. Kearney. 1976. The filterability of normal and leukemic human leukocytes. Blood Cells. 2:491–506.

Needham, D., and R. M. Hochmuth. 1990. Rapid flow of passive neutrophils into a 4 μm pipet and measurement of cytoplasmic viscosity. J. Biomech. Eng. 112:269–276.

Newburger, P. E., and R. T. Parmley. 1991. Neutrophil structure and function. In Hematology. R. Hoffman, E. J. Benz, Jr., S. J. Shattil, B. Furie and H. J. Cohen, editors. Churchill Livingstone, New York. 522–533.

Oppermann, W., and B. Jaberg. 1985. Rheological properties of liver actin solutions. Rheol. Acta. 24:525–529.

Press, W. H., B. P. Flannery, S. A. Teukolsky, and W. T. Vetterling. 1989. Numerical Recipes: The Art of Scientific Computing. Cambridge University Press, New York.

Schmid-Schönbein, G. W., Y. Y. Shih, and S. Chien. 1980. Morphometry of human leukocytes. Blood. 56:866–875.

Schmid-Schönbein, G. W., K-L. P. Sung, H. Tözeren, R. Skalak, and S. Chien. 1981. Passive mechanical properties of human leukocytes. Biophys. J. 36:243–256.

Sheterline, P., and J. E. Rickard. 1989. The cortical actin filament network of neutrophil leukocytes during phagocytosis and chemotaxis. In The Neutrophil: Cellular Biochemistry and Physiology. M. B. Hallett, editor. CRC Press, Boca Raton, FL. 141–165.

Skalak, R., C. Dong, and C. Zhu. 1990. Passive deformation and active motions of leukocytes. J. Biomech. Eng. 112:295–302.

Stossel, T. P. 1984. Molecular architecture of the cytoplasmic matrix. In White Cell Mechanics: Basic Science and Clinical Aspects. H. J. Meiselman, M. A. Lichtman, and P. L. LaCelle, editors. Alan R. Liss, New York. 75–86.

Stossel, T. P. 1988. The mechanical responses of white blood cells. In Inflammation: Basic Principles and Clinical Correlates. J. I. Gallin, I. M. Goldstein and R. Snyderman, editors. Raven Press, New York. 325–341.

Ting-Beall, H. P., D. Needham, and R. M. Hochmuth. 1993. Volume and osmotic properties of human neutrophils. Blood. 81:2774-2780.

Tran-Son-Tay, R., D. Needham, A. Yeung, and R. M. Hochmuth. 1991. Time-dependent recovery of passive neutrophils after large deformation. Biophys. J. 60:856–866.

Tsai, M. A. 1992. Passive mechanical behavior of human neutrophil. Ph.D. thesis. University of Rochester, New York.

Valberg, P. A., and D. F. Albertini. 1985. Cytoplasmic motions, rheology, and structure probed by a novel magnetic particle method. J. Cell Biol. 101:130–140.

Yeung, A., and E. Evans. 1989. Cortical shell-liquid core model for passive flow of liquid-like spherical cells into micropipets. Biophys. J. 56: 139–149.

Zaner, K. S., and T. P. Stossel. 1982. Some perspectives on the viscosity of actin filaments. J. Cell Biol. 93:987–991.

Zaner, K. S., and P. A. Valberg. 1989. Viscoelasticity of F-actin measured with magnetic microparticles. J. Cell Biol. 109:2233–2243.